JUNE 1980

PPPL-1670

UC-20f

EXTERNALLY LAUNCHED ION BERNSTEIN WAVE IN THE ACT-1 TOROIDAL DEVICE

BY

M. ONO AND K. L. WONG

PLASMA PHYSICS LABORATORY

PRINCETON UNIVERSITY
PRINCETON, NEW JERSEY

This work was supported by the U.S. Department of Energy Contract No. DE-AC02-76-CHO 3073. Reproduction, translation, publication, use and disposal, in whole or in part, by or for the United States government is permitted.

Externally Launched Ion Bernstein Wave in the ACT-1 Toroidal Device

Masayuki Ono and King-Lap Wong

Plasma Physics Laboratory, Princeton University
Princeton, New Jersey 08544

ABSTRACT

In a hydrogen plasma (T_e = 2.5 eV, T_i = 1.5 eV), excitation of ion Bernstein waves by an externally placed electrostatic antenna has been investigated for $\omega \simeq 2\Omega_i$. Mode transformation of the electron plasma wave at $\omega \simeq \omega_{pi}$ without observable reflection was observed, followed by strong excitation of the ion Bernstein wave. Detailed measurements of $k_\perp(\omega,k_\parallel)$ and of the wave packet trajectory show excellent agreement with theory.

In ICRF and lower hybrid heating, the importance of mode-conversion (transformation) processes, arising from finite ion-Larmor-radius effects has been recognized for a number of years.[1-5] These processes significantly alter the wave properties near the cold-plasma resonance layer and can profoundly affect the overall efficiencies of these rf heating schemes. Recently it was proposed that a waveguide-launched ion Bernstein wave ($\omega \approx 2\Omega_i$) may offer an attractive alternative method for heating fusion plasmas to ignition temperatures.[6] To achieve wave accessibility, this heating concept invokes mode-transformation of an electron plasma wave into an ion Bernstein wave. In this letter, we report an experiment in an ACT-1 hydrogen toroidal plasma which has provided clear evidence for such mode-transformation at the lower-hybrid resonance layer ($\omega \approx \omega_{pi}$), followed by strong excitation of the $\omega \approx 2\Omega_i$ ion Bernstein waves.

The relevant electrostatic wave dispersion relation for $\omega = \mathcal{O}(\Omega_i)$ can be expressed as[7],

$$k_\perp^2 K_{xx} + k_\parallel^2 K_{zz} = 0 \qquad (1)$$

where

$$K_{xx} = 1 + \sum_\sigma \omega_{p\sigma}^2 \exp(-b_\sigma) b_\sigma^{-1} \sum_{n=1}^{\infty} I_n(b_\sigma)\, 2n^2 (n^2\Omega_\sigma^2 - \omega^2)^{-1}$$

and

$$K_{zz} = 1 + 2 (\omega_{pe}^2/k^2) y^2 [1 + y Z(y)] \approx - (\omega_{pe}^2/\omega^2) \quad ,$$

Here, $b_\sigma \equiv k_\perp^2 T_\sigma/(m_\sigma \Omega_\sigma^2)$, σ designates species, I_n is the modified Bessel function, $y = \omega/k_\parallel (m_e/2\kappa T_e)^{1/2}$, and Z is the

plasma dispersion function. In the low-density edge region where $\omega > \omega_{pi}$, the wave is an electron plasma wave, the dispersion relation for which can be obtained from Eq. (1) in the form

$$n_\perp^2 \simeq - K_{zz}\, n_\parallel^2 \simeq (\omega_{pe}^2/\omega^2)\, n_\parallel^2 . \qquad (2)$$

As the wave propagates from the edge region into the plasma, the finite ion-Larmor-radius effect quickly becomes important[6] and causes transformation of the electron plasma wave into an ion Bernstein wave[8] at the cold-plasma lower-hybrid resonance layer, where $\omega \simeq \omega_{pi}$. To illustrate, we plot, in Fig. 1(a), $k_\perp$ obtained from Eq. (1) vs radial position, using typical ACT-1 parameters. The wave frequency has been chosen so that $\omega/\omega_H \simeq 1.9$ at $r = 0$. Density increases linearly with radial position, r, and when $r \simeq 2$ cm the cold-plasma lower-hybrid resonance condition is satisfied [i.e., $K_{xxo} \equiv K_{xx}\,(T_i = 0) = 1 - \sum_\sigma \omega_{p\sigma}^2/(\omega^2 - \Omega_\sigma^2) = 0$]. The dashed curve shows propagation where $K_{xxo} > 0$, then resonance ($k_\perp^2 \to \infty$) at $K_{xxo} = 0$. The wave is evanescent ($k_\perp^2 < 0$) for $K_{xxo} < 0$. The solid curve presents the warm-ion case ($T_i = 1.5$ eV) showing continuous transformation from an electron plasma wave (EPW) into an ion Bernstein wave (IBW). In Fig. 1(b), the corresponding wave trajectories are shown. As expected for the warm-ion case, the mode-transformation process leads to continuous inward propagation of the wave through the cold-plasma resonance layer.

The experiment was performed in the 5-kiloguass Princeton ACT-1 research torus.[9] Using a hot tungsten-filament source,[9]

a steady-state hydrogen plasma was produced with electron density $n_e \leq 1 \times 10^{11}$ cm^{-3}, electron temperature $T_e \simeq 2.5$ eV, ion temperature $T_i \simeq 1.5$ eV, and plasma radius ~9 cm. The hydrogen neutral pressure in ACT-1 can be reduced to ~7×10^{-6} torr without much reduction in the plasma density, leaving a warm-ion (~1.5 eV) highly ionized (≲50%) hydrogen plasma.[9] Relative ion concentrations were measured using the low-frequency resonance-cone propagation technique;[10] with the present experimental parameters, the measured ion concentrations were 60% H_1^+, 16% H_2^+ and 24% H_3^+. Figure 2(a) shows a schematic of the experimental set-up. Two electrostatic antennas, alternately phased, are placed one port apart (~16.5 cm) at the outer edge (low-field side) of the plasma. This type of electrostatic antenna has been used previously to excite the electron plasma wave[11,12] and also the cold electrostatic ion cyclotron wave.[10] In the present experiment, the excitation frequency was set at $f \simeq 2 f_{ci}(H_1^+) \simeq 12$ MHz, corresponding to $B_o \simeq 4$ kG near the outer plasma edge, and the effective parallel wavelength of the antenna was put at $\lambda_\parallel \simeq 34$ cm so that $\omega/k_\parallel \simeq 4.0 \times 10^8$ cm/sec $>>$ $(2 T_e/m_e)^{1/2} \simeq 1.0 \times 10^8$ cm/sec. The excited waves were detected by rf probes placed at various axial positions.

Figure 2(b) displays radial profiles of the excited wave amplitude for various axial positions, z. The wave launcher is located at r = 0. Inward propagation of the excited wave packet is seen as it travels away from the antenna. The cold-plasma resonance, located at r = 1 cm, causes no visible

perturbation to the wave trajectory. To identify the excited wave, we measured perpendicular and parallel wavelengths by interferometry and in Fig. 3(a) typical radial interferometer patterns are shown for several values of ω/Ω_H. The wave exhibits a cutoff ($\lambda \to \infty$) for $\omega \simeq 2\Omega_H$, and $\lambda_\perp$ decreases with ω/Ω_H. The wavelength also decreases with increasing r (decreasing R) which reduces ω/Ω_H. In Fig. 3(b), where the radial interferometer pattern is shown for various time delays of the boxcar sampler window, the wave phase front moves towards the antenna, confirming the backward propagating nature of the ion Bernstein wave. In Fig. 3(c), we have plotted the measured wave dispersion relation (dots) and find excellent agreement with the theoretical curve for $T_i = 1.5$ eV. The measured parallel wavelength, $\lambda_\parallel \simeq 34$-38 cm, also agrees reasonably well with the effective antenna wavelength, $\lambda_\parallel \simeq 34$ cm. From these measurements we conclude that the excited wave is indeed the ion Bernstein wave.[13,14]

Returning to Fig. 2(b), we have also drawn on this plot ion Bernstein wave trajectories calculated using the experimental parameters. To account for the spread in $\lambda_\parallel$, trajectories are shown for three values of $\lambda_\parallel$. This calculation agrees reasonably well with the observed wave trajectory and explains to some extent the wave packet spreading. The amplitude modulation of the wave packet in Fig. 2(b) is apparently an interference phenomenon perhaps caused by the interaction of the ion Bernstein wave with the near field (electromagnetic component) of the antenna.[15]

In ACT-1, by changing the neutral pressure, the ion temperature can be varied over a wide range (1/40 eV to 2 eV), and Fig. 4(a) shows the interferometer output for several neutral pressures. For the high-pressure case ($p_H = 4 \times 10^{-4}$ torr) the ions are essentially cold ($T_i \simeq 1/40$ eV) and the excited wave is the well-known electron plasma wave[12]; the electron plasma wave excited in this regime behaves quite like the cold-ion case (dashed curves in Fig. 1) where the wave packet stays near the surface, outside of the cold-plasma resonance. As the pressure is reduced (T_i increased), a gradual transformation into the ion Bernstein wave is observed. As may be seen in Fig. 4(a), reduction in pressure causes the ion Bernstein wavelength to increase (recall that $\lambda_\perp \propto \sqrt{T_i}$). In Fig. 4(b), the measured wavenumber (shown as dots) is plotted as a function of the radial position in a warm ion plasma in which the plasma density was lowered so that the cold-plasma resonance occurs at $r \simeq 2$ cm. The solid curve is obtained from Eq. (1) for $T_i = 1.5$ eV, and the dashed curve is for $T_i = 0$. The experimental data agree quite well here with theory, verifying the finite ion-Larmor-radius mode-transformation process.

Efficient mode transformation of the electron plasma wave ($\omega \simeq 2\omega_{ci}$) into an ion Bernstein wave constitutes the central element of a newly proposed method for waveguide-launched rf plasma heating. In an experiment on the ACT-1 torus, this transformation has been observed in considerable detail and the measurements of $k_\perp(\omega, k_\parallel)$ and of the wave-packet trajectories have been found to be in good agreement with theory.

The authors would like to thank T. H. Stix and W. M. Hooke for helpful discussions and continued interest in this work, and J. Taylor, W. Kineyko, and R. Wilson for valuable technical assistance.

This work was supported by the U. S. Department of Energy Contract No. DE-AC02-76-CHO3073.

References

[1]T. H. Stix, Phys. Rev. Lett. 15, 878 (1965).

[2]D. G. Swanson and Y. C. Ngan, Phys. Rev. Lett. 35, 517 (1975).

[3]J. Jacquinot, B. D. McVey, and J. E. Scharer, Phys. Rev. Lett. 39, 88 (1977).

[4]F. W. Perkins, Nucl. Fusion 17, 1197 (1977).

[5]H. Takahashi et al., Phys. Rev. Lett. 39, 31 (1977).

[6]M. Ono, PPPL-1593 (1979).

[7]T. H. Stix, Theory of Plasma Waves (McGraw-Hill, New York, 1962).

[8]D. G. Swanson, Phys. Fluids 10, 1531 (1967).

[9]K. L. Wong and M. Ono, Bull. Am. Phys. Soc. 24, 957, (1979).

[10]M. Ono, Phys. Rev. Lett. 42, 1267 (1979).

[11]R. J. Briggs and R. R. Parker, Phys. Rev. Lett. 29, 852 (1972).

[12]P. M. Bellan and M. Porkolab, Phys. Rev. Lett. 34, 124 (1975).

[13]J. P. M. Schmitt, Phys. Rev. Lett. 31, 982 (1973).

[14]J. P. M. Schmitt and P. Krumm, Phys. Rev. Lett. 37, 753 (1976).

[15]R. K. Fisher and R. W. Gould, Phys. Fluids 14, 857 (1971).

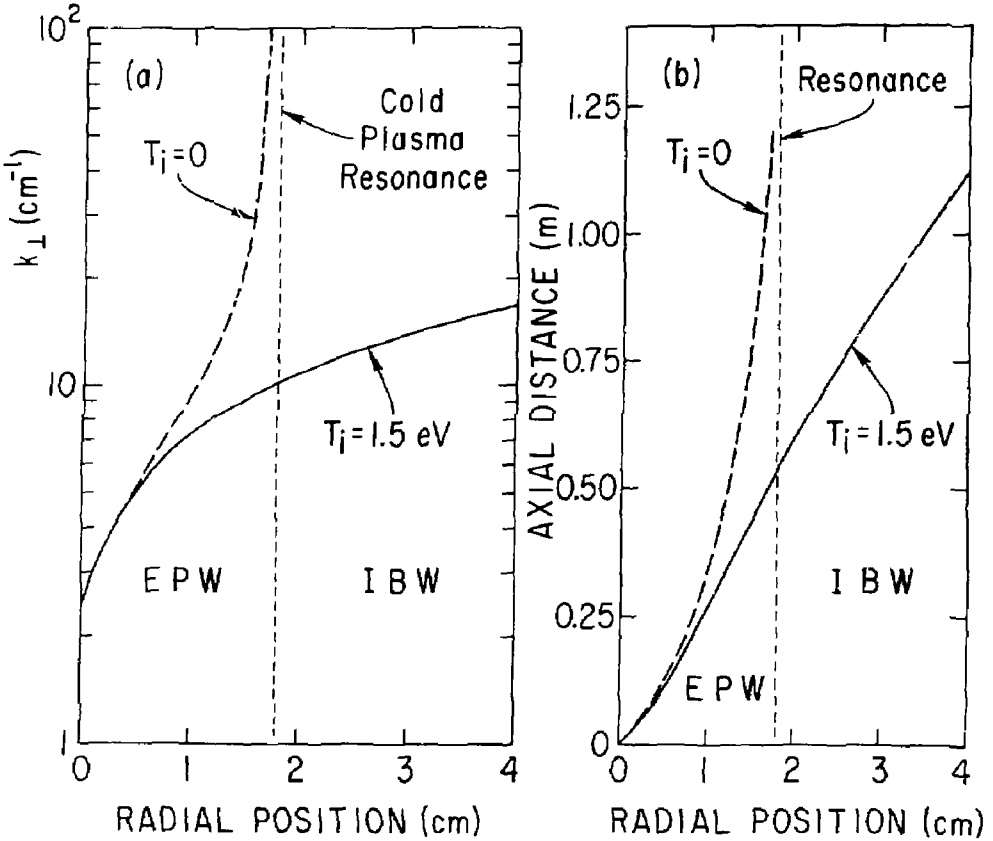

(PPPL-803747)

Fig. 1(a). Wave number vs radial position in a hydrogen plasma with a linear rise in density. F = 12 MHz, ω/ω_H (r = 0)= 1.9, $\lambda_\parallel$ = 34 cm, n_e(res) $\approx$ 2.5 × 10^9cm^{-3}. (b) Wave trajectories for the case shown in Fig. 1(a).

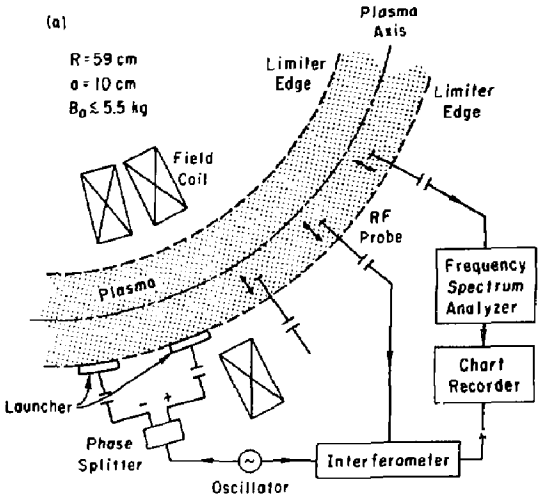

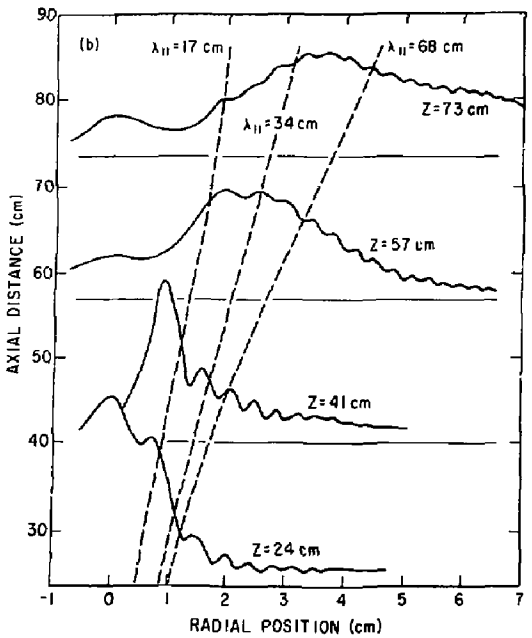

(PPPL-803743)

Fig. 2(a). Schematic of experimental setup. (b) Radial profiles of wave amplitude for various axial position, Z (as labeled). Dashed curves are calculated trajectories.

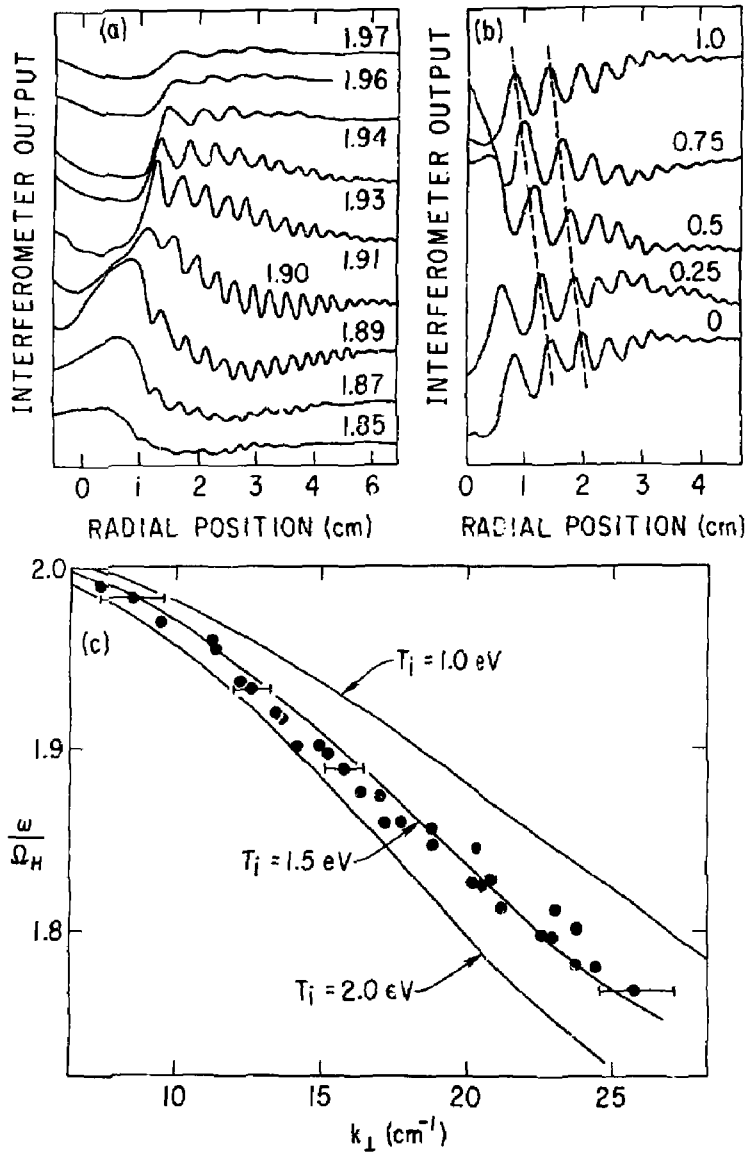

(PPPL-803746)

Fig. 3(a). Interferometer traces. Parameter on each curve is $\omega/\Omega_H(r = 2\ cm)$, f = 12 MHz - 13 MHz, $B_o(r = 2\ cm) \approx 4.3$ kG. (b) Interferometer trace for various time delays, Δt. Parameter on curves is $\omega\Delta t/2\pi$. (c) Wave dispersion relation. Dots are experimental points and solid curves are the theoretical values obtained for various ion temperatures. $p_H = 7.0 \times 10^{-6}$, $n_e = 10^{10}$cm^{-3}.

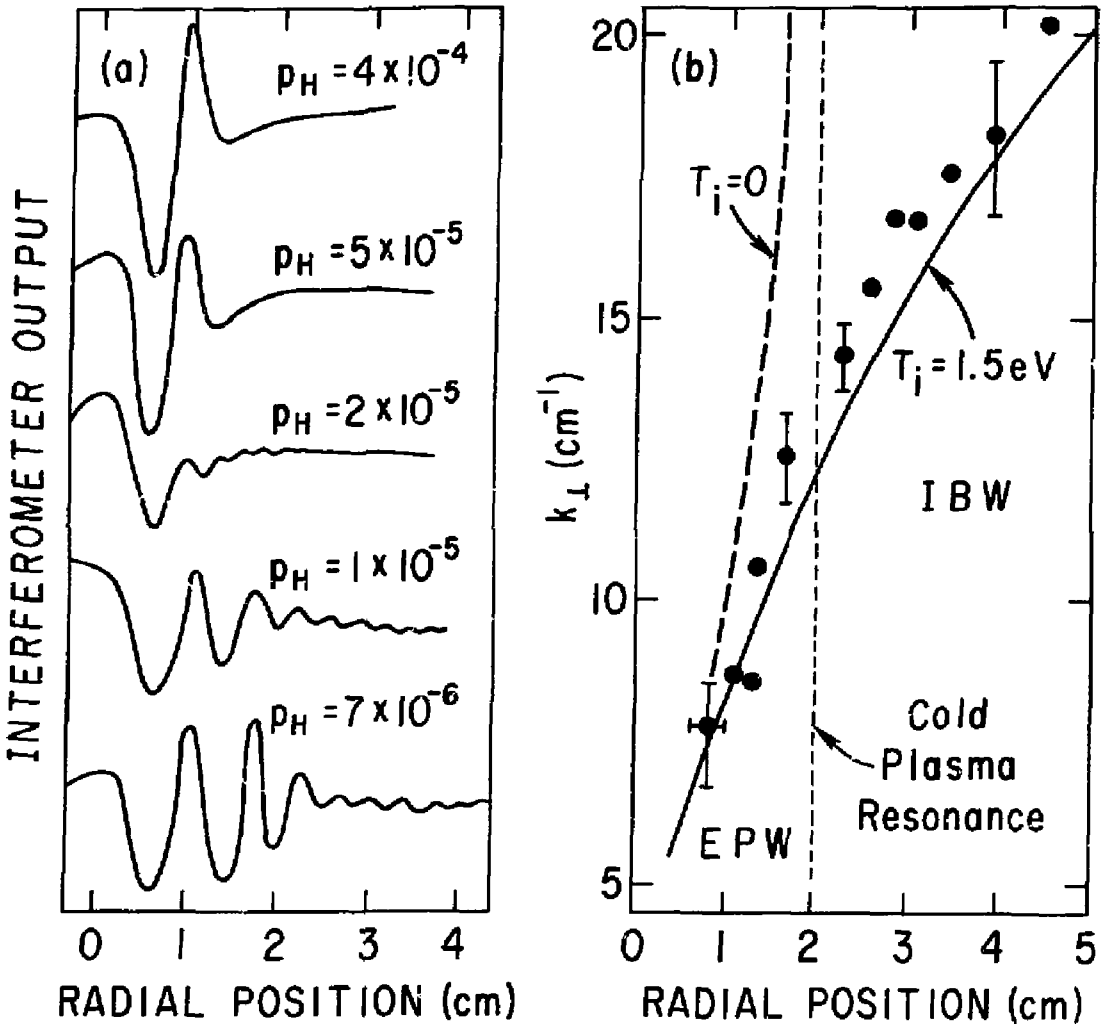

(PPPL-3033745)

Fig. 4(a). Interferometer traces for various neutral pressures. (b) Wave number vs radial position. Dots are experimental points and curves are theoretical values. $\omega/\Omega_H(r = 0) = 1.92$, $p_H = 7 \times 10^{-6}$ torr.